

RSC Advances



This is an *Accepted Manuscript*, which has been through the Royal Society of Chemistry peer review process and has been accepted for publication.

Accepted Manuscripts are published online shortly after acceptance, before technical editing, formatting and proof reading. Using this free service, authors can make their results available to the community, in citable form, before we publish the edited article. This *Accepted Manuscript* will be replaced by the edited, formatted and paginated article as soon as this is available.

You can find more information about *Accepted Manuscripts* in the [Information for Authors](#).

Please note that technical editing may introduce minor changes to the text and/or graphics, which may alter content. The journal's standard [Terms & Conditions](#) and the [Ethical guidelines](#) still apply. In no event shall the Royal Society of Chemistry be held responsible for any errors or omissions in this *Accepted Manuscript* or any consequences arising from the use of any information it contains.



Journal Name

ARTICLE

Improving thermo-electrochemical cell performances by constructing Ag-MgO-CNTs nanocomposite electrodes

Weijin Qian,* Mengjie Li, Lihong Chen, Jianghui Zhang, and Changkun Dong*

Received 00th January 20xx,
Accepted 00th January 20xx

DOI: 10.1039/x0xx00000x

www.rsc.org/

The application of carbon nanotubes (CNTs) as thermo-electrochemical cell (TEC) electrode is still difficult due to its weak contact with the substrate by electrophoretic deposition (EPD) method. In this paper, by doping the suspension of the CNTs with Mg^{2+} and Ag powder, Ag-MgO-CNT nanocomposites were successfully prepared on the stainless steel (SS) substrate by EPD method. The products were confirmed by the characterizations of scanning electron microscopy, X-ray diffraction, energy-dispersive X-ray and X-ray photoelectron spectroscopy. The TEC performances of Ag-MgO-CNT nanocomposite electrodes are much improved due to the higher conductivity, thermal conductivity and better adhesion between the composite films and the SS substrate, depending on the concentrations of Ag powder. The results suggest that constructing Ag-MgO-CNTs nanocomposite electrodes can effectively enhance the performances of CNTs-based TEC, which might be a promising way for the energy harvesting of the CNTs-based TECs by EPD technique.

1 Introduction

To effectively solve the current energy problem, one of the most possible ways is to improve the efficiency of energy conversion by harnessing the waste heat. Thermocells, usually called thermo-electrochemical cells (TECs), were the most effective method to convert thermal energy directly to electrical energy. The sustainable energy source supplied for TECs is mainly from waste heat, eg. waste streams of industry, vehicles exhaust gases, geothermal energy, data storage systems, etc.^{1,2}

Comparing with other solid thermal energy harvesting devices,³⁻⁶ TECs become a promising alternatives for harnessing waste heat due to its easy design, sustained operation, low cost and so on.¹ In order to make TECs more practical, the electrode materials need to be selected with low cost and the relative high conversation efficiency.^{1,7} Traditional catalytic materials, such as platinum and palladium, were used as TEC electrodes because of the high surface catalytic activity for oxidation and reduction reactions.⁸ But the high cost and low conversion efficiency hindered its development. In recent years, Carbon nanomaterials are considered as ideal candidates for TEC electrodes because of its fast electron transfer ability with the potassium ferri/ferrocyanide redox couple.^{1,2,9-16} However, it is difficult to obtain high output power and conversation efficiency for the Carbon nanomaterials with the single-component. Nanocomposites could exhibit intriguing properties due to the synergetic effect of different components that are beneficial for

TECs practical applications.^{7,16} For example, Romano et al. reported that carbon nanotube-reduced graphene oxide composites could achieve much higher conversation efficiency in comparison with the pristine CNTs due to its faster kinetics and larger electroactive surface area.⁷ In addition, the composite electrodes had higher conductivity and specific surface area, which would also result in the better properties for the TECs of the composite electrodes.^{7,16}

The electrophoretic deposition (EPD) technique was widely used to synthesize CNTs-based composites due to its low requirement for substrate's shape, less time-consuming, large-scale production and low cost, etc.¹⁷ Usually, the charging agent, such as $Mg(NO_3)_2$, was added into the electrophoretic suspension to improve the adhesion between CNTs film and the substrate, which is very significant for its practical application.^{18,19} In addition, the charged ions could bring the CNTs to the anode to form the homogeneous film on the substrate.^{19,20} However, the existence of Mg^{2+} would decrease the conductivity of the CNTs due to the formation of MgO after the heat treatment.^{18,19} while Ag-CNTs composites could improve the conductivity and thermal conductivity in comparison with the pristine CNTs²¹⁻²³ and CNTs coated with Ag particles could have also improved its electrochemical properties.²⁴⁻²⁶

Hence, doping CNTs with Mg^{2+} and Ag is expected for the superior TEC performances of the nanocomposites. In this study, we tried to improve the TEC performances of CNTs by doping the electrophoretic suspension of CNTs with Mg^{2+} and Ag powder. The Ag-MgO-CNTs nanocomposite electrodes were constructed by EPD method and the nanocomposite electrodes present much improved TEC performances in comparison with the undoped counterparts, suggesting a promising way for the energy harvesting of CNTs-based TECs by EPD technique.

Institute of micro-nano structure & optoelectronics, Wenzhou University, Wenzhou 325035, P. R. China. Fax: +86 57786689011; Tel.: +86 57786689067; E-mail: weijinqian@wzu.edu.cn, dck@wzu.edu.cn. See DOI: 10.1039/x0xx00000x

2 Experimental

2.1 Synthesis

The Ag-MgO-CNTs nanocomposites were synthesized on the stainless steel (SS) substrate by EPD method. First, the SS substrates were pretreated by acetone, ethanol and purified water for 20 min, respectively. The multiwalled carbon nanotubes (MWNTs, Shenzhen Nanotech. Port Co. Ltd) were washed with acetone and filtered with the purified water, then sonicated in nitric acid for about 20 hours to obtain carboxylic MWNTs.¹⁷ Second, the carboxylic CNTs, MgCl₂ (99.5 %, Aladdin, 0.03 g.L⁻¹, see SI-1 in ESI) and silver powder (99.9%, Aladdin) were dispersed in ethanol and sonicated for about 1 hour to form the suspension. The SS substrate and the counter electrode were immersed into the suspension. After deposition, the products were conducted the annealing process in the furnace at 700°C, then the Ag-MgO-CNTs nanocomposites could be obtained. The TEC performances of the composites could be optimized by adjusting the concentration of Ag in the suspension. The as-prepared composites are denominated as Ag-MgO-CNTs-x, where x represents the concentration of Ag powder.

2.2 Characterization

The morphologies of the products were observed by scanning electron microscopy (SEM; Hitachi S-4800). The species of the products were verified by X-ray diffraction (XRD; GmbH SMART APEX), and the composition analysis were performed by energy-dispersive X-ray analysis (EDS) and X-ray photoelectron spectroscopy (XPS; PHI 5000 VersaProbe).

The tensile tests were conducted by Instron 3343 instrument to evaluate the adhesion between the films (including the pristine CNTs and the Ag-MgO-CNTs nanocomposites) and the SS substrates. First, the sample was fixed by a clamp, subsequently it was wrapped by the tape. During the test, the tape grabbing film was pulled away until the film peeled off from the SS substrate.

Four tungsten needles (about 50µm in diameter) were fixed in line at equal distance. The sample was firstly scraped in part to expose the bare SS substrate for electrical contact test, then it was placed on the platform in contact with the top four needles, and its position could be adjusted to leave the composites film or the CNTs part between the middle two needles. Current was supplied through the outside two needles, and voltage could be obtained by the two middle needles.

2.3 TEC Testing

The TEC performances of the products, such as the short-circuit current (I_{sc}) and the open-circuit potential (V_{oc}) were tested in a U-shaped device. The distance of two test electrodes was 7 cm and the electrode area was 0.36 cm². 0.4M potassium ferri/ferrocyanide (Aladdin) aqueous solution was used as the electrolyte. The temperatures of hot and cold sides were controlled by the heater tape and the recirculation water chiller, respectively. The temperature readings of the two sides were both measured by OMEGA thermocouple probes. The potentials and currents were obtained by the KEITHLEY 2440 multimeter.

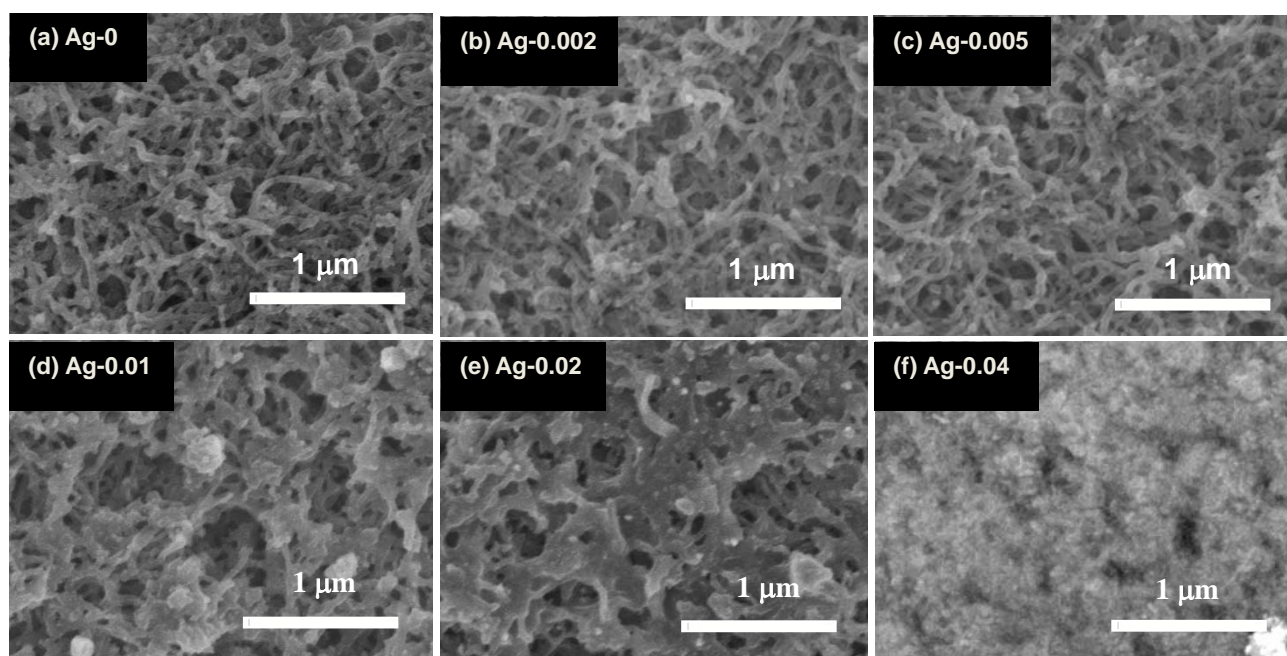


Fig. 1 SEM images of the pristine CNTs and Ag-MgO-CNTs formed with different concentrations of Ag powder. (a) the pristine CNTs; (b-f) the samples obtained by doping 0.002, 0.005, 0.01, 0.02, and 0.04.g.L⁻¹Ag in the suspension, respectively. Note: The concentrations of CNTs and Mg²⁺ were kept certain values with 0.1 and 0.03g.L⁻¹, respectively.

3 Results and discussion

Typical morphologies of the samples are shown in Fig. 1. From the SEM images (Fig. 1a-f), the pristine CNTs sample, with the diameters of 3650 nm, exhibited entanglements (Fig. 1a). As shown in Fig. 1b and 1c, the surface morphology of the CNTs did not show obvious change with the lower concentration of Ag. But with the increasing contents of Ag, (Fig. 1d,e), the surface of CNTs was covered by the agglomerate Ag particles and the surface pastes became more obvious. When the concentration of Ag increased up to 0.04 g.L⁻¹ (Fig. 1f), the surface of the CNTs were almost completely covered by the Ag paste due to the excessive existence of Ag powder, which might result in the decrease in the specific surface area of the CNTs.

XRD and EDS characterizations were applied to confirm the species and compositions of the products. XRD (Fig. 1g) showed the typical reflection peaks at 26.4°, 38.2° and 64.5°, corresponding to the (002) crystallographic planes of CNTs^{27,28} and (111), (200) planes of Ag,^{22,29} respectively. The other four crystallographic planes correspond to SS(110), SS(200), SS(200) and SS(211).³⁰ It is worth mentioning that the reflection peaks of MgO were not observed by XRD, which might be due to the existence of amorphous nature MgO.³¹ EDS result (Fig. 1h) showed the signals of Fe, Cr, C, O, Mg and Ag, as expected. The signals of Fe and Cr are from the stainless steel substrate. O signal are mainly from the MgO due to the heat treatment and MgO could improve the adhesiveness between the composite film and the SS substrate. Ag signal is from Ag powder. The results indicate that the products include CNTs and Ag species.

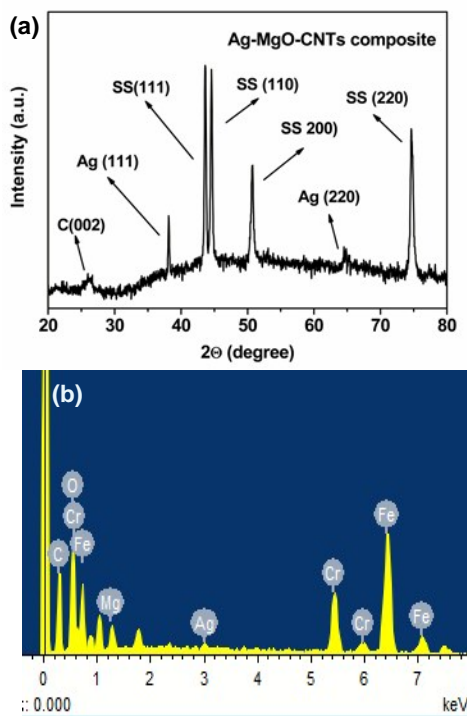


Fig. 2 (a) XRD and (b) EDS results of the Ag-MgO-CNTs-0.01 nanocomposite

Further characterization by XPS exhibited the expected signals from C, O, Mg, and Ag for the nanocomposites, as shown in Figure 3 (also see the Supporting Information, Fig. S2 and Table S1). For the C 1s spectrum (Fig. 3a), a major peak from C-C/C=C bonds were observed at 284.6 eV. In addition, a minor peak from C-O and C=O bonds could be seen at 286.2 and 289.2 eV, respectively.³² As shown in Fig. 3b, the peak from Mg-O bonds was detected at 1303.9 eV for the Mg 1s, which was higher than the peak of metallic Mg (Mg 1s at ~1303 eV).³³ For the O 1s spectrum (Fig. 3c), three peaks at 530.1, 531.7 and 533.3 eV could be assigned to the O-Mg, O-C and O=C bonds, respectively.^{32,34,35} As shown in Fig. 3d, the binding energies (BE) of the Ag 3d_{3/2} and 3d_{5/2} appear at 374.2 eV and 368.2 eV respectively, corresponding to the BE of the metallic silver.^{36,37} The XPS characterization confirmed the existence of MgO and Ag species in the product.

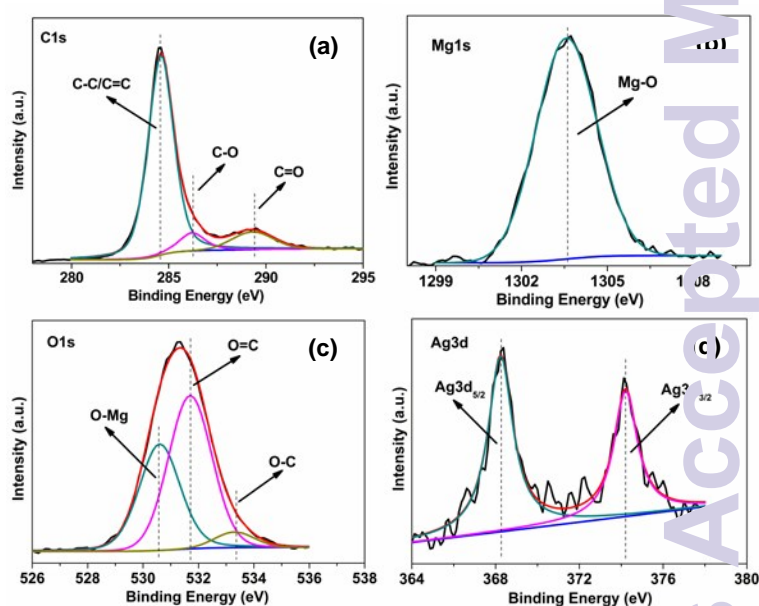


Fig. 3 XPS spectra of the Ag-MgO-CNTs-0.01 sample prepared by EPD. (a) C1s; (b) Mg 1s; (c) O1s; (d) Ag 3d. Note: the peak for C1s at 284.6 eV is used for calibration.

The tensile tests were conducted to investigate the function of CNTs-based films on the adhesion between the films and the SS substrate. We performed the tensile test to measure this adhesion by mechanically pulling away CNT-based films from the SS substrate (see experimental section). As shown in Fig. 4a, the stress curve of the pristine CNTs shows a maximum stress of 0.26 MPa, when doped with Ag powder, the maximum stress of the nanocomposites increase up to 0.32, 0.97, 0.67, 0.62 and 0.48 MPa, corresponding to Ag contents of 0.002, 0.005, 0.01, 0.02 and 0.04 g.L⁻¹, respectively, showing clearly adhesion enhancement with the existence of Ag. Usually, CNTs prepared by EPD have high electrical resistances due to the weak contact between CNTs film and SS substrate.³⁸ In our experiment, Mg²⁺ and Ag powder were added in the CNTs suspension to decrease the electrical resistances of the CNTs electrode. Four-probe device (see experimental) was applied to know the electrical resistance of pristine CNTs and the Ag-MgO-CNTs

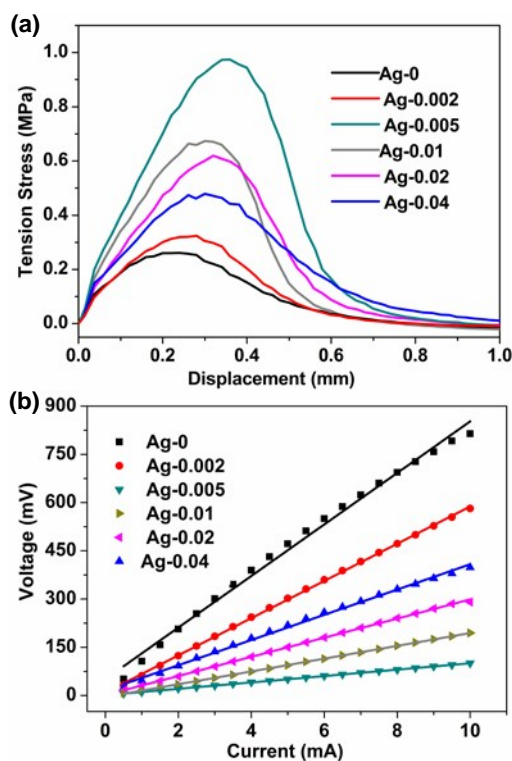


Fig. 4 (a) Tensile tests and (b) Four-probe current–voltage measurements of the pristine CNTs and the Ag-MgO-CNTs nanocomposites

nanocomposites. As shown in Fig. 4b, the resistances of the pristine CNTs electrode was measured to be 80.2Ω , while the resistances of Ag-MgO-CNTs nanocomposite electrodes were measured to be 57.9, 10.0, 19.9, 29.8 and 39.2Ω , corresponding to the Ag concentrations of 0.002, 0.005, 0.01, 0.02 and 0.04 g.L^{-1} , respectively. The results indicate that the surface resistances of the CNTs electrode can be enhanced with the existence of Ag, in agreement with the results of the tensile tests. The resistance of Ag-0.005 is smaller than Ag-0.01, Ag-0.02 and Ag-0.04, mainly due to the two reasons as following. First, the adhesion of the Ag-0.005 sample shows the biggest value compared with other samples (see Fig. 4a), indicating that the good surface contact between the Ag-0.005 sample and the SS substrate. Second, excessive existence of the Ag will lead to the agglomeration of the Ag particles in the samples (see Fig. 1 d-f), which may not be beneficial for the improvement of the conductivity due to the weak synergetic effect of the CNTs-based nanocomposites.

If TECs were continuously operated in an open environment for a long time, the concentration of the electrolyte would be changed due to the solution evaporation, resulting in the instability of the TECs performances. While TECs of closed system could operate with long-term stability.¹ In this work, the U-Shaped TECs (Fig. 5a) of closed system were applied to investigate the TEC performances. As shown in Fig. 5b, the open circuit voltage (V_{oc}) and the temperature difference (ΔT) show the linear relationship.

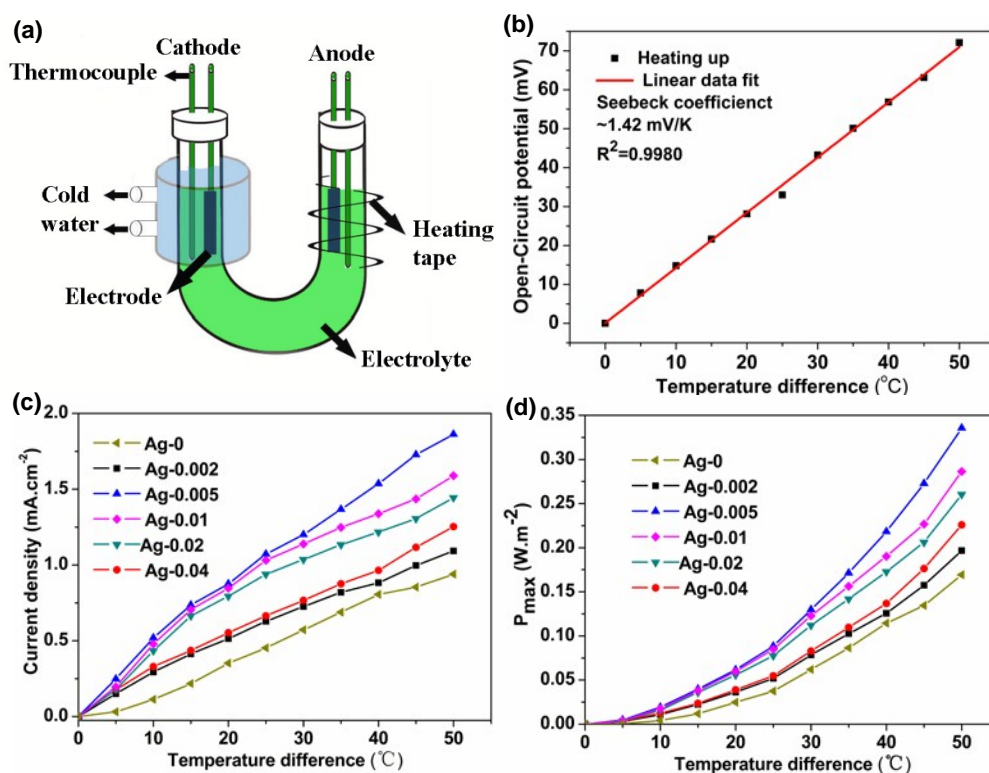


Fig. 5 (a) U-shaped setup for TEC performance measurements, (b) Seebeck coefficient measurements for 0.4 M ferro/ferricyanide redox couple, (c) J_{sc} versus temperature difference between the two test electrodes, (d) P_{max} versus temperature difference.

The seebeck coefficient of the redox couple was usually employed by 0.4M potassium ferro/ferricyanide due to its high seebeck coefficient and large exchange current^{1,7} By linear fitting of data, the seebeck coefficient was obtained ~1.42 mV/k, in agreement with the literatures.^{1,15} Fig. 5c shows that the current densities (J_{sc}) improved with the increasing temperature differences for the pristine CNTs and the nanocomposites, and J_{sc} of the Ag-MgO-CNTs composite electrodes were much higher than that of the pristine CNTs electrode at the same temperature difference, contributed to better conductivity, thermal conductivity, and adhesion between the composite films and the substrate. As for the Ag-MgO-CNTs nanocomposite electrodes, the Ag-MgO-CNT-0.005 nanocomposite shows the best TEC performance, which might be due to the better conductivity, adhesion between the film and the SS substrate and higher specific surface area. When the temperature difference climbed to 50 °C, J_{sc} and $J_{sc}/\Delta T$ reached 9.4 A/m² and 0.19 A/(m²K) for the CNTs electrode, as well as 18.6 A/m² and 0.37 A/(m²K) for Ag-MgO-CNTs-0.005 composite electrode.

To evaluate the performances of the TECs, the maximum output power (P_{max}) and the relative power conversion efficiencies (η_r) are two important parameters. The P_{max} can be described as $0.25V_{oc} \times I_{sc}$. η_r can be expressed as $\eta_r = \eta / (\Delta T / T_h)$ ^{1,13}

$$\eta = \frac{0.25v_{oc} I_{sc}}{Ak(\Delta T / d)}$$

where A is the cross-sectional area of the electrodes, k represents the thermal conductivity of the the redox couple, ΔT and d are the temperature difference and the distance between the test electrodes, respectively, η is the power conversion efficiencies and T_h is the temperature of the hot side. The P_{max} improves with the increasing temperature difference from 5 to 50 °C (Fig. 5d). The P_{max} and η_r for the Ag-MgO-CNT-0.005 electrode are 12.06 μ W and 0.6%, respectively, 100% higher than that for the CNTs electrode, contributed to better conductivity, lower thermal resistance at electrode/substrate junctions.^{1,7} Compared with other nanocomposites electrodes, such as carbon nanotube-reduced graphene oxide (CNTs-rGO), carbon nanotube-activated carbon textiles (C-ACT) (see the Supporting Information, Table S2),^{7,16} TEC performance of Ag-MgO-CNTs-0.005 was not very excellent due to the high thermal resistances of CNTs electrode. To get the optimized output energy from the CNTs-based TEC, the temperature loss between the CNTs electrodes should be considered.¹ In order to solve this problem, one of the most effective ways is to minimize the thermal resistance of the CNTs electrodes. In our experiment, the thermal resistance at the MWNT film/substrate junction was 0.0611 cm²K/W under the CNTs electrode thickness of 500 μ m, higher than the previous reports.^{1,39} Further research should be devoted to improving the performances of the CNTs-based TEC by decreasing the thermal resistance of the junction, e.g., try to improve the thermal conductivity of the junction by reducing the electrodes thickness or selecting the single wall CNTs as the electrodes.^{1,40} In addition, taking into account the low η_r

of the CNTs-based TEC, it is necessary to design the series or flowing TECs.^{1,11}

4 Conclusions

In summary, the Ag-MgO-CNTs nanocomposites have been successfully prepared by EPD method and have been confirmed by different characterizations. The TEC performances of Ag-MgO-CNTs nanocomposite electrodes show much improvement due to the higher conductivity, thermal conductivity and better adhesion between the composite films and the SS substrate, depending on the concentrations of the Ag powder. The results indicate that constructing Ag-MgO-CNTs nanocomposite electrodes can effectively improve the TEC performances of CNTs, which might offer a promising way for promoting the energy harvesting of CNTs-based TECs by EPD technique.

Acknowledgements

This work was financially supported by National Science Foundation of China (No. 11274244, 51302193).

Notes and references

- R. C. Hu, B. A. Cola, N. Haram, J. N. Barisci, S. Lee, S. Stoughton, G. Wallace, C. Too, M. Thomas, A. Gestos, M. E. D. Cruz, J. P. Ferraris, A. A. Zakhidov and R. H. Baughman, *Nano Lett.*, 2010, 10, 838-846.
- T. J. Kang, S. L. Fang, M. E. Kozlov, C. S. Haines, N. Li, Y. H. Kim, Y. S. Chen, and R. H. Baughman, *Adv. Funct. Mater.*, 2012, 22, 477-489.
- C. B. Vining, *Nat. Mater.*, 2009, 8, 83.
- T. Mancini, P. Heller and B. J. Butler, *Sol. Energy Eng.*, 2003, 125, 135.
- M. Ujihara, G. P. Carman and D. G. Lee, *Appl. Phys. Lett.*, 2007, 91, 093508.
- D. A. W. Barton, S. G. Burrow and L. R. Clare, *J. Vib. Acoust.*, 2010, 132, 021009.
- M. S. Romano, N. Li, D. Antiohos, J. M. Razal, A. Nattestad, S. Beirne, S. L. Fang, Y. S. Chen, R. Jalili, G. G. Wallace, R. Baughman and J. Chen, *Adv. Mater.*, 2013, 25, 6602-6606.
- T. I. Quickenden and Y. Mua, *J. Electrochem. Soc.*, 1995, 142, 3985.
- T. J. Abraham, D. R. MacFarlane and J. M. Pringle, *Chem. Commun.*, 2011, 47, 6260.
- T. J. Abraham, N. Tachikawa, D. R. MacFarlane and J. M. Pringle, *Phys. Chem. Chem. Phys.*, 2014, 16, 2527.
- P. F. Salazar, S. Kumar and B. A. Cola, *J Appl Electrochem.*, 2014, 44, 325-336.
- T. J. Abraham, D. R. MacFarlane and J. M. Pringle, *J. Chem. Phys.*, 2011, 134, 114513.
- S. Manda, A. Saini, S. Khaleeq, R. Patal, B. Usmani, S. Harinipriya, S. Pratiher and B. Roy, *J. Mater. Res. Technol.*, 2013, 2, 165-181.
- M. F. El-Kady, V. Strong, S. Dubin and R. B. Kaner, *Science*, 2012, 335, 1326.

ARTICLE

Journal Name

- 15 L. Tang , Y. Wang , Y. Li , H. Feng , J. Lu and J. Li , *Adv. Funct. Mater.*, 2009 , 19 , 2782 .
16. H. Im, H. G. Moon, J. S. Lee, I. Y. Chung, T. J. Kang and Y. H. Kim. *Nano Research*, 2014, 7, 443–452.
- 17 A. R. Boccaccini , J. Cho , J. A. Roether , B. J. C. Thomas , E. J. Minay and M. S. P. Shaffer, *Carbon*, 2006, 44, 3149–3160.
- 18 A. A. Talin., K. A. Dean, S. M. O'Rourke, B. F. Coll, M. Stainer and R. Subrahmanyam, US Patent, 2005, 6902658.
- 19 S. Oh, J. Zhang, Y. Cheng, H. Shimoda and O. Zhou. *Appl. Phys. Lett.*, 2004, 84, 3738–3740.
- 20 H. Zhao, H. Song, Z. Li, G. Yuan and Y. Jin, *Appl. Surf. Sci.*, 2005, 251, 242–244.
- 21 L. F. Chen, H. Q. Xie and W. Yu. *J Mater Sci.*, 2012, 4, 5590–5595.
- 22 R. X. Dong, C.T. Liu, K.C. Huang, W.Y. Chiu, K.C. Ho and J. J. Lin, *ACS Appl. Mater. Interfaces*, 2012, 4, 1449–1455.
- 23 F. Xin and L. Li, *Composites: Part A*, 2011, 42, 961–967.
- 24 P. Yang, W. Wei, C. Tao, B. Xie and X. Chen, *Microchim. Acta*, 2008, 162, 51.
- 25 G.Y. Gao, D. J. Guo, C. Wang, and H. L. Li, *Electrochem. Commun.*, 2007, 9, 1582–1586
- 26 D. J. Guo and H. L. Li, *Carbon*, 2005, 43, 1259–1264.
- 27 N. Jha and S. Ramaprabhu, *J. Appl. Phys.*, 2009, 106, 084317.
- 28 H. K. Kim, K. C. Roh, K. Kang and K.B. Kim, *RSC Adv.*, 2013, 3, 14267–14272.
- 29 R. Mendoza-Reséndez, A.Gómez-Treviño, E. D. Barriga-Castro, N.O. Núñez and C. Luna, *RSC Adv.*, 2014, 4, 1650–1658.
- 30 A. K. De, D.C. Murdock , M. C. Mataya , J. G. Speer and D. K. Matlock. *Scripta Mater.*, 2004, 50, 1445–1449.
- 31 S. K. Mahadeva , J. C. Fan , A. Biswas, K. S. Sreelatha , L. Belova and K. V. Rao, *Nanomaterials*, 2013, 3, 486–497.
- 32 T. I. T. Okpalugo, P. Papakonstantinou, H. Murphy, J. McLaughlin, N. M. D. Brown, *Carbon*, 2005, 43, 153 – 161.
- 33 J. S. Corneille, J. W. He and D. W. Goodman, *Surf. Sci.*, 1994, 36, 269–278.
- 34 X. B. Yan, T. Xu, S. R. Yang, H. W. Liu, Q. J. Xue, *J. Phys. D: Appl. Phys.*, 2004, 37, 2416–2424.
- 35 G. Carta, N. E. Habra, L. Crociani, G. Rossetto, P. Zanella, A. Zanella, G. Paolucci, D. Barreca and E. Tondello, *Chem. Vap. Deposition*, 2007, 13, 185–189.
- 36 G. A. Gelves, B. Lin, U. Sundararaj and J. A. Haber, *Adv. Funct. Mater.*, 2006, 16, 2423 – 2430.
- 37 S. H. Lee, C. C. Teng, C. M. Ma and I. Wang, *J. Colloid Interf. Sci.*, 2011, 364, 1–9.
- 38 Y. R. Chen, H. Jiang, D. B. Li, H. Song, Z. M. Li, X. J. Sun, G. Q. Miao and H. F. Zhao, *Nanoscale Res. Lett.*, 2011, 6, 537.
- 39 B. A. Cola, J. Xu, C. Cheng, X. Xu, H. Hu and T. S. Fisher, *J. Appl. Phys.* 2007, 101, 054313.
- 40 M. Fujii, X. Zhang, H. Q. Xie, H. Ago, K. Takahashi, T. Ikuta, H. Abe and T. Shimizu, *Phys. Rev. Lett.*, 2005, 95, 065502.